ACI STRUCTURAL JOURNAL TECHNICAL PAPER

Title No. 116-S17

Drift Capacity of Reinforced Concrete Structural Walls with Special Boundary Elements

by Saman A. Abdullah and John W. Wallace

Performance of reinforced concrete (RC) walls in recent laboratory tests and in recent strong earthquakes has revealed that thin wall boundaries are susceptible to concrete crushing, reinforcing bar buckling, and lateral instability. To address this concern, a wall database with detailed information on more than 1000 tests was assembled to enable the study of the impact of various parameters on wall deformation capacity. For this study, the data are filtered to identify and analyze a dataset of 164 tests on well-detailed walls generally satisfying ACI 318-14 provisions for special structural walls. The study indicates that wall deformation capacity is primarily a function of the ratio of wall neutral axis depth-to-compression zone width (c/b), the ratio of wall length-to-compression zone width (l_w/b), wall shear stress ratio ($v_{max}/\sqrt{f_c'}$), and the configuration of boundary transverse reinforcement. Based on these observations, an expression is developed to predict wall drift capacity with low coefficient of variation.

Keywords: compression zone width; cross-sectional aspect ratio; drift capacity; overlapping hoops; structural wall; wall shear stress.

INTRODUCTION

Reinforced concrete (RC) structural walls are commonly used as lateral force-resisting elements in tall and moderately tall buildings because they provide substantial lateral strength and stiffness and are assumed to provide the needed nonlinear deformation capacity if detailed according to ACI 318. Major updates to ACI 318 design provisions for slender walls occurred in 1983, 1999, and 2014. In 1983, an extreme compression fiber stress limit of $0.2f_c'$ under bending and axial stress was introduced to determine if special boundary transverse reinforcement was required, whereas in 1999, an alternative to the stress-based approach, a displacement-based approach, was introduced to evaluate the need for special boundary transverse reinforcement for slender, continuous walls. In 2014, more stringent detailing requirements for slender ($h_w/l_w \geq 2.0$) walls were introduced to address issues associated with detailing and lateral stability of thin walls, and to include a minimum wall thickness for sections that are not tension-controlled. The ACI 318-83 provisions were based on research conducted by the Portland Cement Association (PCA) (Oesterle et al. 1976 and 1979) and Paulay and Goodsir (1985), which demonstrated that large lateral drift ratios could be achieved when compression zones in yielding regions were adequately detailed to remain stable, whereas the 1999 additions were based primarily on the work by Wallace and Moehle (1992), Wallace (1994), and Thomsen and Wallace (2004) to develop a displacement-based approach to assess wall boundary detailing requirements. The 2014 changes to ACI 318 were based on observations from recent earthquakes and laboratory tests (Wallace 2012; Wallace et al. 2012; Nagae et al. 2011; Lowes et al. 2012).

Even with the 2014 updates, the underlying premise of the ACI 318-14 approach to design and detailing of special structural walls is that walls satisfying the provisions of Sections 18.10.6.2 through 18.10.6.4 possess drift capacities in excess of the expected drift demands. However, recent research has shown that wall drift capacity is impacted by wall geometry, configuration of boundary transverse reinforcement, and level of wall shear stress. For example, Segura and Wallace (2018a) studied the relationship between wall thickness and lateral drift capacity and found that thin walls possess smaller lateral drift capacities than thicker walls that are otherwise similar. Furthermore, it has been found that thin, rectangular sections confined by an outer hoop and intermediate legs of crossties, which is a detail allowed by ACI 318-14, Section 18.10.6.4, at wall boundaries, is less stable in compression than sections that use overlapping hoops for confinement (Welt 2015; Segura and Wallace 2018a). Finally, Whitman (2015) suggested, using finite element analysis, that the confined length of a boundary element should be increased over that currently required, to address the increase in compression demands that result from higher shear demands.

This research focuses on assessing which wall design parameters have the greatest impact on wall lateral drift capacity by assembling a detailed database that includes data from more than 1000 large-scale tests. The data are filtered to identify a dataset of 164 tests on walls that are ACI 318-14 code-compliant, or nearly code-compliant, and results for these tests are analyzed. The data analysis is then used to develop an expression to predict mean wall drift capacity prior to substantial lateral strength loss with low coefficient of variation (COV).

RESEARCH SIGNIFICANCE

Recent research has indicated that wall lateral drift capacity is significantly impacted by wall geometry, detailing, and compression and shear stress demands; however, current ACI 318-14 provisions do not adequately address the role of these parameters on wall drift capacity. Instead, it is assumed that all walls satisfying requirements of ACI 318-14 (Sections 18.10.6.1 through 18.10.6.4) possess adequate drift capacity to meet the estimated drift demands

ACI Structural Journal, V. 116, No. 1, January 2019.

MS No. S-2017-460.R1, doi: 10.14359/51710864, was received December 13, 2017, and reviewed under Institute publication policies.

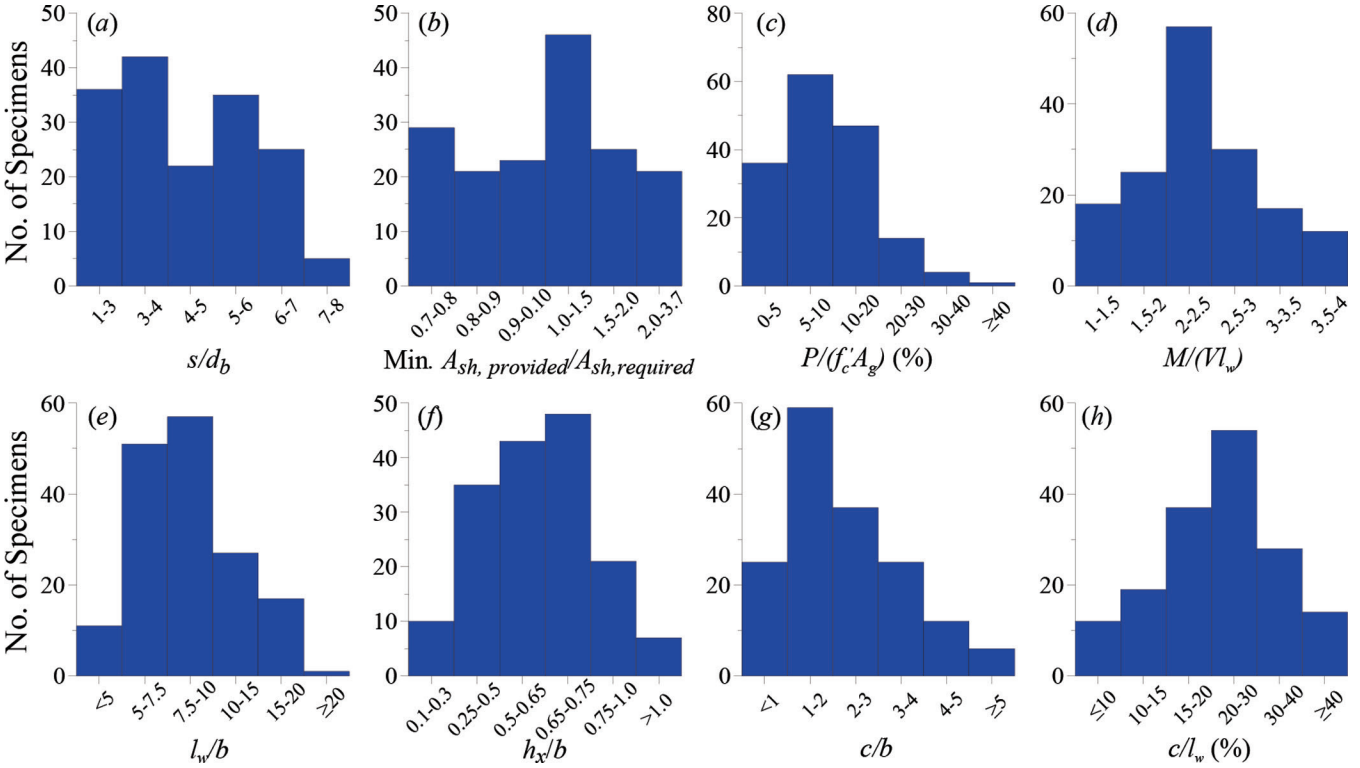

Fig. 1—Histograms of dataset (164 tests) used in this study.

determined from analysis. A test database is assembled and analyzed to study the impact of various design parameters and derive an expression for the lateral drift capacity of slender walls with ACI 318-14 special boundary elements.

EXPERIMENTAL RC WALL DATABASE

Prior to the mid-1990s, relatively few large-scale experimental studies had been conducted on relatively slender reinforced concrete structural walls (Oesterle et al. 1976, 1979; Paulay and Goodsir 1985). However, since then, a substantial number of experimental studies have been conducted to assess the impact of various design parameters on wall load-deformation responses and failure modes. Several attempts have been made to assemble wall databases (for example, NEEShub Shear Wall Database [Lu et al. 2010], and the SERIES Database 2013) to assist in the development of code provisions and to validate analytical models for RC walls; however, these databases do not contain sufficient information to allow detailed and robust assessment of wall lateral drift capacity. In addition, a significant number of tests have been conducted since the 2010 Chile and 2011 New Zealand earthquakes, and data from these more recent tests are typically not included in these databases. To address these issues, a new database was developed, referred to as UCLA-RCWalls, which includes information from more than 1000 wall tests from more than 200 experimental programs reported in the literature. The database includes detailed information about the tests—that is, wall cross-section, loading protocol, configuration of boundary transverse reinforcement, and material properties. The database also includes backbone relations (base shear-total top displacement, base moment-base rotation, and/or base shear-top shear displacement), consisting of seven points (origin, cracking, general yielding, peak, ultimate, residual, and collapse). Ultimate deformation capacity is defined as the total displacement or rotation at which strength degrades 20% from the peak strength, which has been widely used to define deformation at strength loss (Elwood et al. 2009). Finally, the database also contains analytical (or computed) data such as moment-curvature relationships, nominal and yield moment strength M_n and M_y, and curvature ϕ_n and ϕ_y; neutral axis depth c and wall shear strength computed according to ACI 318-14.

An important aspect of the database involved addressing the impact of different test setups (cantilever wall tests [Thomsen and Wallace 2004], versus panel/partial height wall tests [Segura and Wallace 2018a]) on wall lateral drift capacity. For the wall panel tests and partial wall height tests, the UCLA-RCWalls database includes the drift capacity at the effective height $M_{u,base}/V_{u,base}$, determined as the sum of the measured displacement at the top of the panel (experimental) and the estimated contribution of elastic bending deformations between the top of the test specimen and the effective height (Segura and Wallace 2018b).

For this study, which focuses on the drift capacity of walls with special boundary elements (SBEs), the UCLA-RCWalls database was filtered to include only wall tests satisfying the following requirements:

(a) Quasi-static, reversed cyclic loading;

(b) Measured concrete compressive strength, $f_c' \geq 3$ ksi (20.7 MPa);

(c) Ratio actual tensile-to-yield strength of boundary longitudinal reinforcement $f_u/f_y \geq 1.2$;

Table 1—Correlation coefficients, *R*, for design parameters and wall drift capacity

Design parameter	c/b	l_w/b	$v_{max}/\sqrt{f_c'}$	$P/A_g f_c'$	$A_{sh,provided}/A_{sh,required}$	s/d_b	h_x/b	$\rho_{long.BE}$	$\rho_{t,web}$*	f_u/f_y	l_{BE}/l_w*	c/l_w	$l_w c/b^2$
Correlation coefficient, *R*	–0.66	–0.56	–0.30	–0.08	0.13	–0.02	–0.25	–0.32	–0.14	–0.07	0.06	–0.32	–0.68

*$\rho_{t,web}$ is web transverse reinforcement ratio; l_{BE}/l_w is length of confined boundary normalized by wall length.

(d) Rectangular, or nearly rectangular, compression zone b;

(e) Wall web thickness $t_w \geq 3.5$ in. (90 mm);

(f) A minimum of two curtains of web vertical and horizontal reinforcement;

(g) Shear span ratio, $M/Vl_w \geq 1.0$;

(h) Boundary longitudinal reinforcement ratio $\rho_{Long,BE} \geq 6\sqrt{f_c'(\text{psi})} / f_y[0.5\sqrt{f_c'(\text{MPa})} / f_y]$;

(i) Ratio of provided-to-required (per ACI 318-14, Section 18.10.6.4) area of boundary transverse reinforcement, $A_{sh,provided}/A_{sh,required} \geq 0.7$;

(j) Ratio of vertical spacing of boundary transverse reinforcement to minimum diameter of longitudinal boundary reinforcement $s/d_b \leq 8.0$;

(k) Centerline distance between laterally supported boundary longitudinal bars h_x, between 1.0 and 9.0 in. (25 and 230 mm); and

(l) Reported strength loss due to flexural tension or compression failure—that is, tests were excluded if some noticeable strength loss was not observed (only three tests were excluded for this reason), or if walls exhibited shear (for example, diagonal tension, diagonal compression, and sliding at the base) or lap slice failures prior to yielding of longitudinal reinforcement.

Based on the selected filters, a total of 164 test specimens were identified. Histograms for various database parameters for the 164 tests are shown in Fig. 1, where $P/(A_g f_c')$ is the axial load is normalized by concrete compressive strength f_c' and gross concrete area A_g; and M/Vl_w is the ratio of base moment-to-base shear normalized by wall length l_w. The filters were selected to identify walls that satisfied, or nearly satisfied, ACI 318-14, Chapter 18 provisions for special structural walls, including requirements for boundary transverse reinforcement in Section 18.10.6.4. A concrete compression strength limit of 3 ksi (20.7 MPa) was specified in accordance with requirements of ACI 318-14 Section 18.2.5 for special seismic systems. Walls with web thickness t_w, less than 3.5 in. (90 mm) were not included because use of two layers of web reinforcement along with realistic concrete cover is not practical. At least two curtains of web reinforcement were specified to be consistent with ACI 318-14 Section 18.10.2.2. The limit on ratio f_u/f_y is slightly less restrictive than the limit of 1.25 specified in ACI 318-14 Section 20.2.2.5. The specified limits on $s/d_b \leq 8.0$ and $A_{sh,provided}/A_{sh,required} \geq 0.7$ are slightly less restrictive than the current limits in ACI 318-14 Section 18.10.6.4 of 6.0 and 1.0, respectively, to include more data. The limit on $\rho_{Long.BE}$ was included to avoid brittle tension failures (Lu et al. 2016). ACI 318-14, Section 18.10.6.4e, requires $h_{x,max}$ not exceeding the lesser of 14 in. (355 mm) or $2b/3$; however, most of the tests in the database were conducted at 25 to 50% scale; therefore, $h_{x,max}$ for the wall tests should generally be between 3.5 and 7.0 in. (89 and 178 mm) for the 14 in. (355 mm) limit. Based on the range of h_x used to filter the data, 95% of the specimens have $h_x \leq$ 6 in. (152 mm), which is reasonable, whereas the histogram for h_x/b presented in Fig. 1(f) indicates that a majority of tests have $h_x/b < 3/4$, which is slightly higher than the current limit of $h_x/b < 2/3$.

The histogram for the parameter M/Vl_w, presented in Fig. 1(d), indicates that 44 tests in the reduced database have $1.0 \leq M/Vl_w < 2.0$ and 120 tests with $M/Vl_w \geq 2.0$. Tests with $M/Vl_w \geq 2.0$ are generally appropriate for assessing the drift capacity of walls designed using ACI 318-14, Section 18.10.6.2, which requires $M/Vl_w \geq 2.0$, whereas the other tests are more appropriate for walls designed according to ACI 318-14, Section 18.10.6.3. Walls with $M/Vl_w <$ 1.0 are not included because they are generally governed by shear failure. In subsequent assessments presented herein, either the entire dataset of 164 tests is used, or subsets for $1.0 \leq M/Vl_w < 2.0$ and $M/Vl_w \geq 2.0$ are used, as deemed appropriate.

In ACI 318-14, Eq. (18.10.6.2), roof drift demand δ_u/h_w determined using ASCE 7 analysis procedures is used to assess the need for SBEs; however, no specific check is required to ensure that the roof drift capacity of a wall with SBEs exceeds the roof drift demand. An alternative approach to use plastic rotation was not considered in this study because ACI 318-14 does not include a definition for plastic hinge rotation and plastic hinge rotation capacities from wall tests are not always measured in tests or reported in the literature. However, it would be a relatively simple task to covert roof drift to rotation (elastic and plastic) over an assumed plastic hinge length. To facilitate comparison of test drift capacities with drift demands determined from analysis, drift capacities for the 164 tests corresponding to the effective height $h_{eff} \approx 0.7h_w$ were adjusted to determine roof level h_w drift ratios to be consistent with ACI 318-14, Eq. (18.10.6.2), which uses roof level drift demand to assess the need for special boundary elements. To accomplish this task, the increase in elastic drift between h_{eff} and h_w was estimated analytically based on the ASCE 7-10 Section 12.8 equivalent lateral force procedure for a Class B site in Los Angeles with number of stories estimated based on h_{eff} (Fig. 2) and an approximate test scale. The wall effective bending stiffness between h_{eff} and h_w was determined at first yield of boundary longitudinal reinforcement based on a computed moment-curvature relation included in the database. Use of this approach typically increased the elastic roof level displacements by 10 to 20%, which is relatively

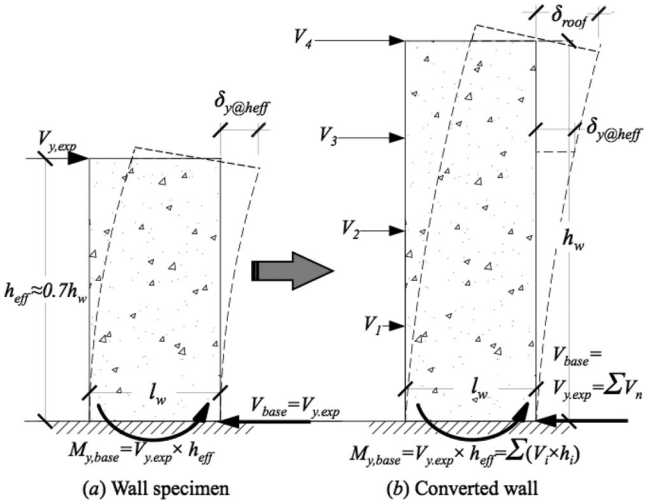

Fig. 2—Conversion of elastic drift from h_{eff} *and* h_w.

small compared to nonlinear displacements, which are due to plastic hinge rotation at the wall base, and thus nonlinear drift at h_{eff} and h_w are equal.

PARAMETERS THAT IMPACT WALL LATERAL DRIFT CAPACITY

Parameters likely to impact the lateral drift capacity of walls with SBEs (Table 1) were selected based on a review of current codes/standards and available literature (ACI 318-14; ASCE 41-13; Oesterle et al. 1976 and 1979; Brown et al. 2006; Birely 2012; Segura and Wallace 2018a). Based on this review, the following parameters were expected to have the greatest impact on wall lateral drift capacity: 1) ratio of wall neutral axis depth-to-width of the compression zone c/b, where c is computed for an extreme fiber concrete compressive strain of 0.003; 2) ratio of the wall length-to-width of the compression zone l_w/b; 3) ratio of the maximum wall shear stress ratio $v_{max}/\sqrt{f_c'}$; and 4) the configuration of the boundary transverse reinforcement used—that is, use of overlapping hoops versus a single perimeter hoop with intermediate crossties. Other parameters investigated (Table 1) did not significantly impact wall lateral drift capacity, as will be shown in subsequent paragraphs.

A series of linear regression analyses were performed to identify the most influential parameters, on wall drift capacity. Correlation coefficients R, for the complete dataset of 164 tests for various parameters are presented in Table 1. Parameters c/b, l_w/b, and $v_{max}/\sqrt{f_c'}$ produce the highest correlation coefficients with wall drift capacity, with R being 0.66, 0.56, and 0.30, respectively. A similar approach indicated that use of overlapping hoops versus a single perimeter hoop with supplemental legs of crossties impacted lateral drift capacity. Other parameters, such as $\rho_{Long.BE}$, h_x/b, and c/l_w produce modest R-values; however, the impact of these parameters are already incorporated into c/b and l_w/b. Other parameters, within the range of the filtered data, had little impact on lateral drift capacity. A more detailed assessment of the four more significant parameters is presented in the following paragraphs by using results from companion tests and results from the dataset of 164 tests. Following this presentation, a general expression to predict wall drift capacity is presented that includes the influence of these four parameters.

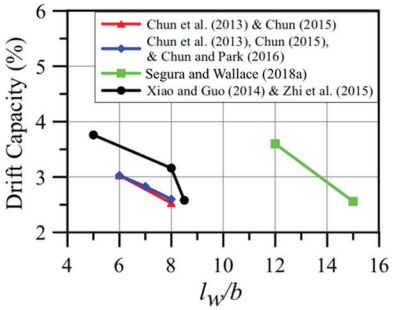

Fig. 3—Drift capacity of companion specimens against cross section slenderness ratio.

Impact of l_w/b

Brown et al. (2006) assembled a building inventory of post-1991 designed mid-rise buildings using structural walls as the primary lateral load resisting system on the west coast of the United States. The building inventory indicated that walls with $l_w/b \geq 15$ are quite common; however, due to limitations associated with laboratory testing, it is noted that there are only a handful of test specimens (six tests) with SBEs and very slender cross sections $l_w/b \geq 20$ in the selected dataset, as seen from Fig. 1(e). The complete database of more than 1000 tests includes 38 tests with $l_w/b \geq 20$; however, 32 of them do not meet the filtering criteria for the reduced dataset because they either failed in shear, did not have sufficient boundary transverse reinforcement, or were tested under monotonic loading.

Although the linear regression analysis indicated a fairly strong correlation between l_w/b and drift capacity, various parameters are changing and it is not always clear which variables are impacting drift capacity. Therefore, the reduced dataset (164 tests) was examined to find companion tests—that is, tests where the change in ratio l_w/b is due to changes of primarily one parameter at a time (either wall length l_w or wall compression zone width b). Results for drift capacity versus l_w/b are presented in Fig. 3 for four series of companion test specimens with SBEs (Chun 2015; Chun and Park 2016; Chun et al. 2013; Segura and Wallace 2018a; Xiao and Guo 2014; Zhi et al. 2015) and indicate substantial reductions in wall drift capacity. The reason for this is not obvious. For example, consider two cantilever walls constructed with the same materials and of the same height h_w pushed to the same top displacement $\delta_u > \delta_y$ with identical values of wall length l_w, neutral axis depth c/l_w, and wall shear stress $v_{max}/\sqrt{f_c'}$, where l_w/b is varied by only changing b. For this to be the case, wall longitudinal reinforcement would have to be changed to maintain the ratios of c/l_w and $v_{max}/\sqrt{f_c'}$ as b changes. Because yield displacement (that is, associated with first yield of boundary longitudinal reinforcement) is related to c/l_w, the yield displacements are equal, and therefore, the inelastic displacements are equal. Based on the common assumption that wall plastic hinge length l_p, is related to wall length l_w—that is, $l_p = 0.5l_w$, and assuming plane sections remain plane after loading (which has been shown to be reasonably true, refer to Thomsen

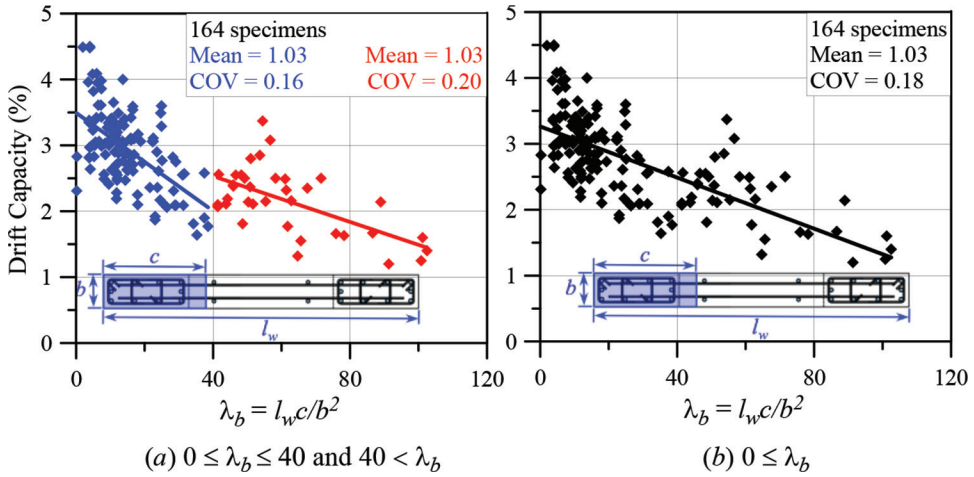

Fig. 4—Wall drift capacity variation versus λ_b.

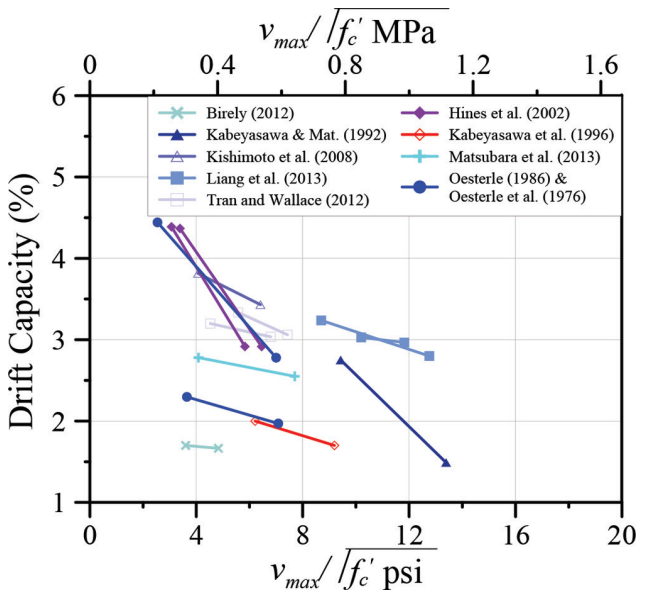

Fig. 5—Companion specimens with special detailing and different levels of wall shear stress.

and Wallace 2004), then the strain gradient along the cross section at all locations would be identical. Under these conditions and assumptions, there is no reason to expect that the drift capacities of the two walls should be different. The one important parameter that is not constant in this example is the ratio of neutral axis depth to the wall compression zone thickness c/b. Segura and Wallace (2018b) has shown that, for slender walls that fail due to flexural compression (concrete crushing, reinforcement buckling, and lateral instability of the compression zone), ratio c/b is as shown in the subsequent section, an important variable as the compressive strains tend to concentrate over a wall height that is more closely related to b than l_w. The walls tested by Segura and Wallace (2018a) have similar drift capacities to the other companion test specimens presented in Fig. 3, which have lower values of l_w/b, because other parameters are influencing drift capacity, as mentioned previously and discussed as follows.

Impact of *c/b*

Segura and Wallace (2018b) show that larger values of c/b impact drift capacity because thicker walls increase the spread of plasticity and provide increased lateral stability under nonlinear compression yielding. Takahashi et al. (2013) observed that c/b correlates well with plastic drift capacity for slender walls with modest boundary transverse reinforcement. The histogram plotted in Fig. 1(g) indicates that only 18 tests have been conducted with $c/b > 4$.

As noted previously in Table 1, use of a combined slenderness parameter $\lambda_b = (l_w/b)(c/b)$ provided an efficient means to account for slenderness of the cross section l_w/b and the slenderness of the compression zone on the cross section c/b. This combined parameter, as noted previously, considers the impact of concrete and reinforcement material properties, axial load, wall geometry, and quantities and distributions of longitudinal reinforcement at the boundary and in the web. Figure 4 and Table 1 indicate that wall drift capacity is strongly correlated with λ_b, with drift capacity varying between 1.25 and 3.25% as λ_b reduces from 80 to 0. The cluster of data points with $\lambda_b \approx 80$ includes the tests by Birely (2012), which have a rather slender cross section $l_w/b \approx 20$ and a relatively large ratio of $c/b \approx 4$ to 5, although the ratio of $c/l_w \approx 0.20$ to 0.25 is not vastly different than many other tests included in the dataset (refer to Fig. 1).

The results plotted in Fig. 4 have very important design implications. For design level shaking (DE), ASCE 7-10 Section 12.12.1 limits allowable interstory drift ratio to 0.02 for typical RC buildings in Risk Category I and II that are taller than four stories and use structural walls as a lateral-force-resisting system. At maximum considered earthquake (MCE) level shaking, which is commonly used to assess collapse prevention, this limit is typically taken as 0.03. If roof drift is approximated as three-quarters of peak interstory drift, then the peak roof drift demand allowed by ASCE 7-10 is approximately 0.0225. Results presented in Fig. 4 indicate that the drift capacities of RC walls with SBEs vary substantially—that is, all RC walls with SBEs do not have the same drift capacity, and walls with $\lambda_b > 50$ have a mean drift capacity less than that allowed by ASCE 7-10. Results are presented for two ranges of λ_b in Fig. 4(a) and for the entire dataset in Fig. 4(b), to show that trends are similar.

Table 2—Companion wall specimens with special detailing and different levels of wall shear stress

Reference	Test ID	$P/A_g f_c'$, %	M/Vl_w	$\rho_{long.BE}$, %	$V_{n,ACI}/A_{cv}\sqrt{f_c'}$ in psi	$V_{test}/A_{cv}\sqrt{f_c'}$ in psi	$V_{@Mn}/A_{cv}\sqrt{f_c'}$ in psi	c/l_w, %	l_w/b	c/b	Drift capacity, %
Kishimoto et al. (2008)	No. 5	18.3	2.0	4.0	7.2	6.4	5.7	35	8.0	2.8	3.43
	No. 6	17.7	3.0			4.1	3.7				3.82
Kabeyasawa and Matsumoto (1992)	NW-1	10.9	2.0	2.1	8.9	9.4	7.5	20	8.5	1.7	2.75
	NW-2	10.2	1.3		9.6	13.4	10.9				1.49
Liang et al. (2013)	DHSCW-02	21.0	2.1	2.7	9.3	8.7	8.9	34	5.0	1.7	3.24
	DHSCW-04		1.5		9.7	12.8	12.4	33		1.6	2.80
Tran and Wallace (2015)	RW-A20-P10-S38	7.3	2.0	3.0	4.4	4.5	3.6	17	8.0	1.4	3.20
	RW-A20-P10-S63			6.7	6.7	6.8	6.1	22		1.7	3.04
Tran and Wallace (2015)	RW-A15-P10-S51	7.7	1.5	3.0	5.9	5.6	4.9	18	8.0	1.4	3.34
	RW-A15-P10-S78	6.4		5.7	8.2	7.4	6.9	21		1.7	3.06
Hines et al. (2002)	1A	9.3	4.0	1.6	7.6	3.4	2.8	20	4.5	0.9	4.37
	2A	9.7	2.0		7.9	6.5	5.8				2.92
Hines et al. (2002)	1B	8.3	4.0	1.6	3.6	3.1	2.7	20	4.5	0.9	4.39
	2B	8.5	2.0			5.8	5.4				2.92
Kabeyasawa et al. (1996)	HW1	–8.0	2.3	4.3	7.2	6.2	4.1	12	11	1.3	2.00
	HW2	–7.9	2.0			9.2	6.1	17		1.9	1.70
Matsubara et al. (2013)*	N	4.5	1.5	1.6	7.5	7.7	6.2	22	14.5	3.2	2.55
	N(M/Qd3.1)	5.3	3.1	1.5	7.1	4.1	3.1	24		3.5	2.78
Oesterle (1986)	R3	6.9	2.4	5.9	7.3	7.1	6.1	25	18.7	4.7	1.97
	R4	7.4		3.4	6.1	3.6	3.5	19		3.6	2.30
Oesterle et al. (1976)	B3	0.0	2.4	1.1	4.6	2.5	2.3	5	6.3	0.3	4.44
	B5			3.7	7.6	7.0	6.2	10		0.6	2.78
Liang et al. (2013)*	DHSCW-01	28.0	2.1	2.7	10.0	10.2	10.0	46	5.0	2.3	3.03
	DHSCW-03	21.0	1.5			11.8	12.5	34		1.7	2.97
Birely (2012)*	PW1	9.5	2.8	3.4	4.9	3.6	3.2	22	20	4.3	1.70
	PW2	13.0	2.2		4.7	4.8	4.6	25		5.1	1.66

*Although these specimens were intended to be companion specimens, there is a moderate variation between the two specimens.

Notes: $V_{n,ACI}$ is nominal wall shear strength in accordance with ACI 318-14, Section 18.10.4; $V_{@Mn}$ is wall shear strength corresponding to nominal flexural strength M_n; 1 ksi = 1000 psi = 6.895 MPa.

The findings suggest strongly that changes to ACI 318-14 are needed to address this issue. A possible approach to address this issue would be to include a drift demand versus drift capacity provision in ACI 318, for example, similar to demand-to-capacity checks for moment or shear strengths, or drift capacity of slab-column connections (ACI 318-14, Section 18.14.5), to meet a specified level of reliability.

Impact of $v_{max}/\sqrt{f_c'}$

As noted earlier, wall shear stress demand, expressed as $v_{max}/\sqrt{f_c'}$, has a significant impact on wall lateral drift capacity, where $v_{max} = V_{max}/A_{cv}$ and V_{max} is taken as the maximum shear force that develops in the wall where yielding of tension reinforcement under combined bending and axial stresses limits the shear force demand, and $A_{cv} = l_w \times t_w$. It is noted that, because the database includes only walls tested under quasi-static loading, the impact of dynamic shear amplification is not considered (Keintzel 1990; Eberhard and Sozen 1993). Even for relatively slender walls, which are defined in ACI 318-14 as $h_w/l_w \geq 2.0$, there is ample evidence that wall lateral drift capacity is impacted by shear, for example, refer to experimental studies presented in Fig. 5 and Table 2 and trends shown in Fig. 6(b). Kolozvari et al. (2015) used a shear-flexure interaction model to demonstrate that shear transfer from diagonal compressive struts into the flexural compression zone results in higher concrete compressive strains than would result from bending and axial load alone, and also tends to increase the neutral axis depth modestly. As well, ASCE 41-13 Tables 10-19 and 10-21 include wall modeling parameters (for example, plastic rotation capacities at lateral strength loss and at axial failure) that depend on the level of wall shear stress, with values of $4\sqrt{f_c'}$ and $6\sqrt{f_c'}$ psi ($0.33\sqrt{f_c'}$ and $0.5\sqrt{f_c'}$ MPa) for walls with lower and higher shear demands, respectively. Currently, ACI 318-14 Section 18.10.4.4 allows wall shear stress demands as high as $10\sqrt{f_c'}$ psi ($0.83\sqrt{f_c'}$ MPa) for individual wall segments, although the average shear stress demand on walls resisting a common shear force is limited to $8\sqrt{f_c'}$ psi ($0.67\sqrt{f_c'}$ MPa).

As was done earlier for parameter l_w/b, the impact of shear stress on wall lateral drift capacity is first evaluated

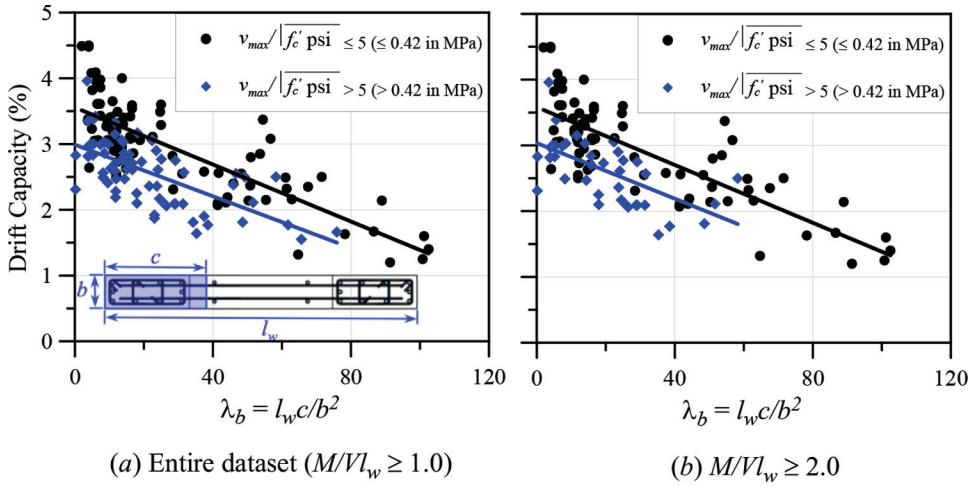

Fig. 6—Impact of wall shear stress on wall drift capacity.

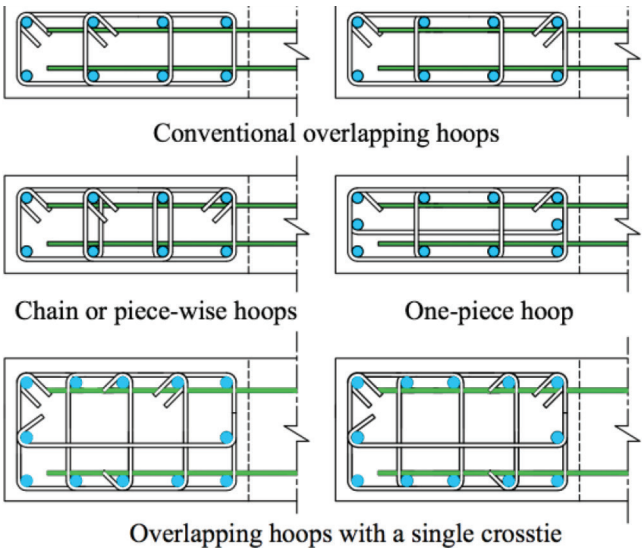

Fig. 7—Types of overlapping hoop configurations observed in database.

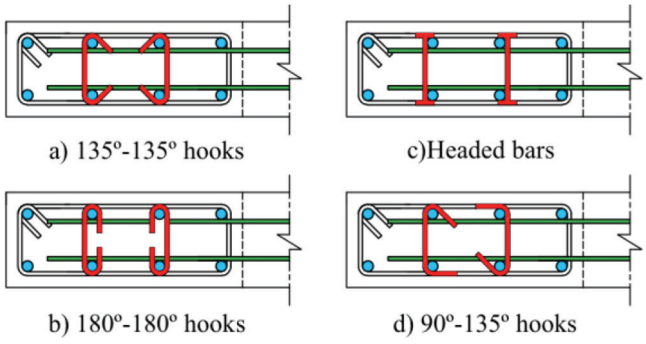

Fig. 8—Types of crossties observed in database.

by using companion tests, where the primary test variable is wall shear stress. In general, for the companion specimens, a change in shear stress demand was accomplished by either varying M/Vl_w or the quantity of longitudinal reinforcement (refer to programs presented in Table 2); for this latter condition, in addition to shear stress, wall moment capacity and neutral axis depth are also impacted. Figure 5 shows wall drift capacity versus shear stress ratio (that is, $v_{max}/\sqrt{f_c'}$) for 13 pairs of companion specimens and indicates that higher shear demands have a detrimental impact on wall drift capacity, even for relatively low shear demands—that is, $v_{max}/\sqrt{f_c'}$ psi ≤ 5 ($v_{max}/\sqrt{f_c'}$ MPa ≤ 0.42). Table 2 provides detailed information about the results plotted in Fig. 5. It also is noted that the impact (slope) of shear stress is different from one pair of companion specimens to another, indicating that other parameters may also be at play (for example c/b, because increasing this ratio also tends to reduce drift capacity). Drift capacities versus λ_b are plotted in Fig. 6(a) for the entire dataset (164 tests) with $M/Vl_w \geq 1.0$ and in Fig. 6(b) for the slender walls (120 tests) in the dataset with $M/Vl_w \geq 2.0$ to demonstrate that shear stress demand impacts drift capacity beyond what can be attributed to changes in other variables. The tests are separated into two bins, one for low-to-modest and the other for higher shear stress demands. The trend lines plotted in Fig. 6(a) and (b), which are offset by approximately 0.5% drift, clearly indicate that higher shear demand has a significant negative impact on wall drift capacity. Therefore, it is appropriate that the level of shear stress demand on a wall should be considered when assessing drift capacity, which is consistent with ASCE 41-13 Table 10-19, where the modeling parameters and acceptance criteria vary with level of wall shear stress.

Overlapping hoops

As noted earlier, one of the primary reasons to develop the database was to assess the impact of different detailing options on wall drift capacity. ACI 318-14, Section 18.7.5.2a, states that "transverse reinforcement shall comprise either single or overlapping spirals, circular hoops, or rectilinear hoops with or without crossties"; therefore, both configurations are allowed and are assumed to be equivalent. To assess the impact of overlapping hoops on lateral drift capacity, very detailed information on the configuration of boundary transverse reinforcement used in each test was included in the database. Different types of overlapping hoop configurations observed in the database are shown in Fig. 7, whereas different configurations used for supplemental crossties

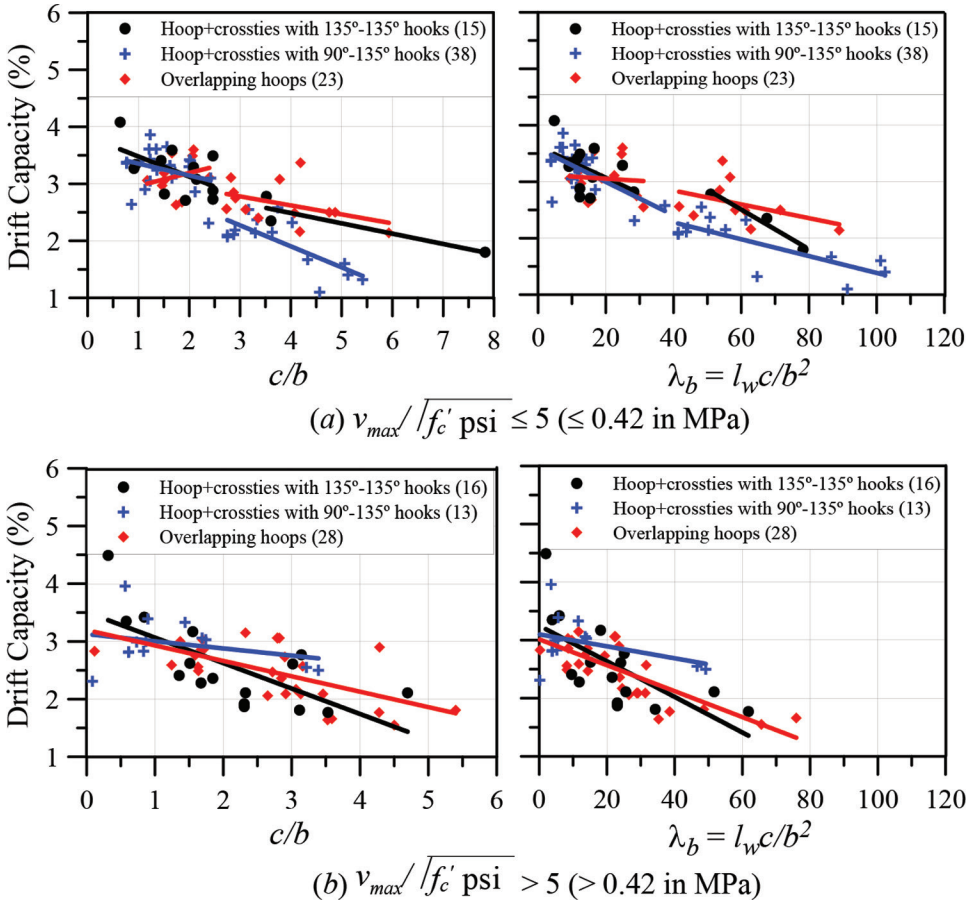

Fig. 9—Comparison of different boundary transverse reinforcement configurations. (Note: number of tests for each case is given in parentheses).

combined with a single perimeter hoop are shown in Fig. 8. It is noted that ACI 318-14, Section 25.3.5, requires that crossties shall have a seismic hook (135 degrees) at one end and a 90-degree hook at the other end, and that the 90-degree hooks on successive crossties engaging the same longitudinal bars must be alternated end for end vertically and along the perimeter of the boundary element. For columns, ACI 318-14, Section 18.7.5.2, requires use of seismic hooks (135 degrees) on both ends of crossties for high axial load ratios and high concrete compressive strengths (f_c' ≥ 10,000 psi [69 MPa]); however, this provision does not apply to walls. As noted in Fig. 8, a range of crosstie configurations are included in the database. Tests with 135- to 135-degree hooks on crossties were primarily conducted in Japan, where the Architectural Institute of Japan (AIJ 2010) requires their use, and China. Test results that use a single perimeter hoop with headed bar crossties for wall boundary transverse reinforcement (Fig. 8(c)) are limited to the studies by Mobeen (2002) and Seo et al. (2010). However, walls tested using headed bars for crossties have relatively small ratios of l_w/b and c/b, such that $\lambda_b \leq 6$ and strength degradation for these tests resulted from longitudinal bar fracture; therefore, these tests, by themselves, do not provide sufficient insight into the effectiveness of headed bars used for transverse reinforcement within SBEs.

Of the 164 tests, analysis of the dataset indicates that 51 tests used overlapping hoop configurations such as those shown in Fig. 7, whereas 51 and 31 tests used a combination of a perimeter hoop and crossties with 90- to 135-degree hooks and 135- to 135-degree hooks, respectively. Twenty-eight tests used a single hoop without intermediate legs of crossties, and the rest (3 tests) used headed bars as intermediate legs combined with a single perimeter hoop such as that shown in Fig. 8(c); however, these three tests have $c/b \leq 1.3$ and $\lambda_b \leq 6$. Drift capacity versus c/b and λ_b, for $v_{max}/\sqrt{f_c'}$ psi ≤ 5 [$v_{max}/\sqrt{f_c'}$ MPa ≤ 0.42] and $v_{max}/\sqrt{f_c'}$ psi > 5 [$v_{max}/\sqrt{f_c'}$ MPa > 0.42] are shown in Fig. 9(a) and (b), respectively. For the lower shear stress range, use of overlapping hoops provides improved drift capacity of, $c/b \geq 2.5$ or $\lambda_b \geq 40$ (Fig. 9(a)), whereas the use of a perimeter hoop with 135- to 135-degree crossties results in only a slight increase in drift capacity over the use of 90- to 135-degree crossties. It is noted that, for $c/b \geq 2.5$, the provided length of confinement was, on average, 118% of that required by ACI 318-14, which is defined as at least the greater of $c - 0.10l_w$ and $c/2$; therefore, the test results in the database were not significantly overdesigned with respect to length of confinement provided. The phenomenon of "90-degree hook opening prematurely" for walls with larger λ_b ratios has been observed in recent laboratory programs (Birely 2012), with approximately $80 \leq \lambda_b \leq 100$ and Segura and Wallace (2018a), with approximately $45 \leq \lambda_b \leq 60$. For the Segura and Wallace (2018b) tests, $2.0 \leq c/b \leq 4.0$ and $0.2 \leq c/l_w \leq 0.3$. Observations indicated that once cover concrete spalled and longitudinal bar buckling initiated, crosstie hooks opened and the long leg of the perimeter hoop was ineffective in resisting the forces exerted on it by

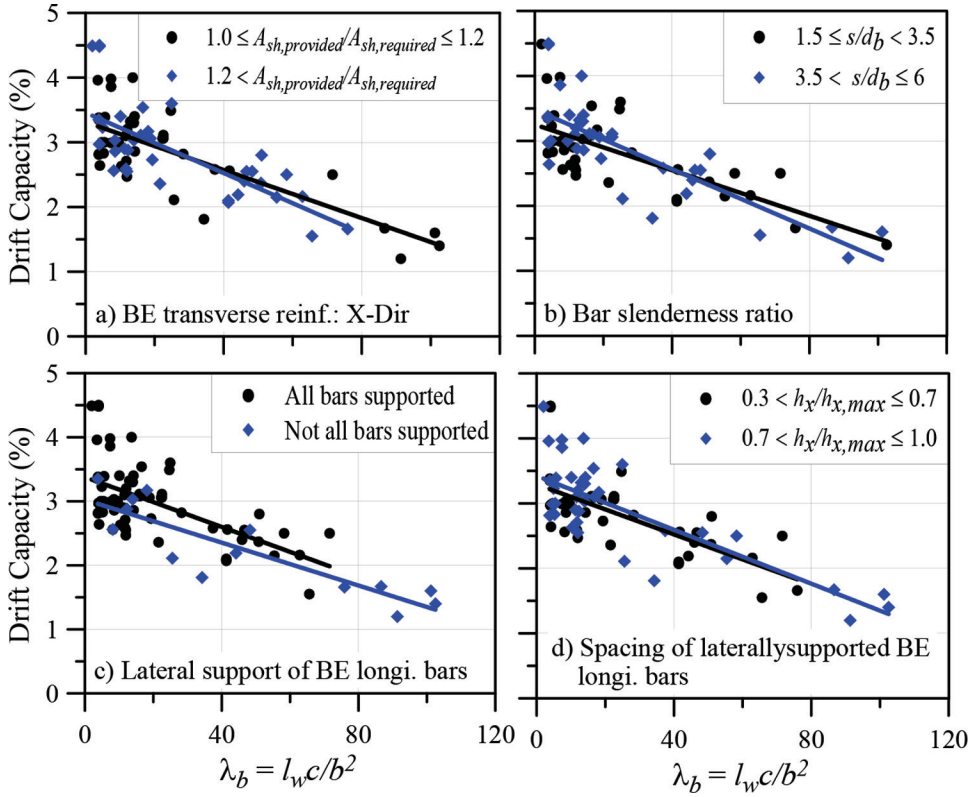

Fig. 10—Impact of some boundary element details on drift capacity of walls with SBEs.

the buckling longitudinal reinforcement, leading to concrete crushing of the core of the SBE and subsequent lateral instability of the boundary. For values of $\lambda_b \geq 50$, use of overlapping hoops results in a 50 to nearly 100% increase in drift capacity (Fig. 9(a)). Interestingly, use of overlapping hoops for the tests with high shear stresses—that is, $v_{max}/\sqrt{f_c'}$ psi > 5 ($v_{max}/\sqrt{f_c'}$ MPa > 0.42) does not indicate a clear trend of increased drift capacity (Fig. 9(b)); however, it is noted that relatively few tests exist for $\lambda_b \geq 40$ to evaluate this trend. Given these observations, it would seem prudent to require the use of overlapping hoops for ratios of $c/b \geq 2.5$; alternatively, the impact of the reduced drift capacity of the wall could be accounted for in the design process. This issue is addressed later.

Other factors

As noted earlier, the primary variables impacting wall lateral drift capacity were c/b, l_w/b, $v_{max}/\sqrt{f_c'}$, and configuration of the boundary transverse reinforcement used. However, for completeness, the influence of other variables on lateral drift capacity is presented herein to demonstrate that they do not significantly impact lateral drift capacity. Parameters considered include: 1) minimum $A_{sh,provided}/A_{sh,required}$; 2) s/d_b; 3) $h_x/h_{x,max}$; 4) degree of lateral support provided (support for all boundary longitudinal bars versus every other bar); and 5) $P/A_g f_c'$. For these variables, the dataset of 164 tests was further reduced to include only those tests that fully satisfy the ACI 318-14 provisions, particularly those related to quantities $A_{sh,provided}$, s, s/d_b, h_x, and l_{be}, resulting in a reduced dataset of 78 code-compliant wall test specimens. Results are discussed in subsequent paragraphs.

Results presented in Fig. 10(a) indicate that providing ratios of $A_{sh,provided}/A_{sh,required}$ modestly greater than 1.0, does not significantly increase wall lateral drift capacity. Similarly, results presented in Fig. 10(b) demonstrate that variations in s/d_b (and s) also have little influence on wall lateral drift capacity, particularly for the practical range of $3 \leq s/d_b \leq 6$, suggesting that the current ACI 318-14 limits are sufficient. Additional investigation indicated no significant difference in drift capacity trends for $3 \leq s/d_b \leq 4$ and $4 < s/d_b \leq 6$. Comparison of test results where lateral support was provided for every boundary longitudinal bar by corners of a crosstie or hoop leg versus for every other longitudinal boundary bar (for example, Fig. 10(c)), indicates only a slight improvement in drift capacity when all bars are supported, although data are limited for $\lambda_b > 60$ for configurations where all bars are supported. It is noted that, for columns with high axial load $P_u > 0.3A_g f_c'$ or high concrete strength ($f_c' \geq 10{,}000$ psi [69 MPa]), ACI 318-14 Section 18.7.5.42(f) requires that every longitudinal bar around the perimeter of a column have lateral support provided by the corner of a hoop or by a seismic hook, and the value of h_x cannot exceed 8 in. (200 mm). For wall with SBEs, ACI 318-14, Section 18.10.6.4(e), requires h_x not exceed the least of 14 in. (356 mm) or $2b/3$. The 14 in. (356 mm) limit governs only for relatively thick walls ($b \geq 21$ in. [533 mm]); no walls within the reduced database fell into this category. Figure 10(d) indicates that, for the range of h_x within the dataset (that is, $0.3 \leq h_x/h_{x,max} \leq 1.0$), and assuming an average test scale factor of 40% for all tests, $h_{x,max}$ = 0.4 x 14 in. = 5.6 in. (142 mm), variations in h_x had no impact on wall drift capacity. An alternative approach, where h_x was normalized to the wall compression

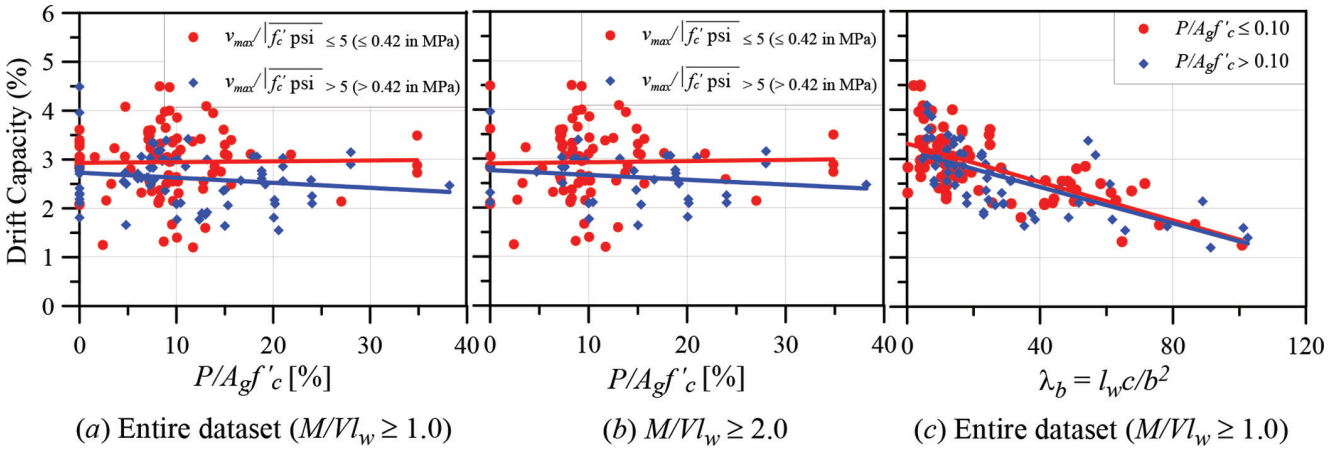

Fig. 11—Impact of axial load ratio $P/A_g f_c'$ *on drift capacity of walls with SBEs.*

zone width b, did not alter the trends noted in Fig. 10(d). Based on the information provided herein, requiring wall SBEs to satisfy the same requirements (ACI 318-14, Section 18.7.5.2(f)), for columns with high axial load $P_u > 0.3A_g f_c'$ or high concrete strength ($f_c' \ge 10{,}000$ psi [69 MPa]) would be expected to only slightly improve wall lateral drift capacity. However, as noted, due to the lack of data, adding such a requirement might be prudent.

Axial load is typically assumed to have a significant impact on wall (or column) lateral drift (or plastic rotation) capacity. For example, in UBC 1997 Section 1921.6.6.3 and ASCE 41-13 Section 10.7.1.1, if axial load on a wall exceeded $0.3A_g f_c'$, the lateral strength of the wall could not be considered. Additionally, ASCE 41-13 Tables 10-19 and 10-20 use axial load ratio as a primary term for selecting modeling parameters and acceptance criteria for both flexure- and shear-controlled walls. However, as noted earlier in Table 1, axial load ratio by itself had no clear correlation with wall drift capacity (correlation coefficient, $R = 0.08$). Variation of wall drift capacity against axial load ratio $P/A_g f_c'$ is shown in Fig. 11(a) for the entire dataset with $M/Vl_w \ge 1.0$ and in Fig. 11(b) for slender walls in the dataset with $M/Vl_w \ge 2.0$, whereas trends for two levels of $P/A_g f_c'$ are shown in Fig. 11(c). From Fig. 11, it is clear that there is no significant trend between axial load ratio (ranging from 0.0 to 0.35) and wall drift capacity. It is noted that the slenderness parameter λ_b described earlier incorporates the impact of axial load through neutral axis depth.

DRIFT CAPACITY PREDICTION

A primary objective of this study was to develop an empirical model to predict lateral drift capacity of structural walls with SBEs. Key variables impacting lateral drift capacity have been identified, such as, $\lambda_b = l_w c/b^2$, $v_{max}/\sqrt{f_c'}$, and the use of overlapping hoops versus a single perimeter hoop with intermediate legs of crossties. Other variables also were investigated and found to not substantially influence lateral drift capacity for cases were ACI 318-14 detailing provisions for SBEs are satisfied. It is important to note herein that the authors are not saying that these parameters do not influence lateral drift capacity, defined as a 20% drop in strength from the peak lateral load, only that changes in these parameters within ranges that are permissible or reasonable for

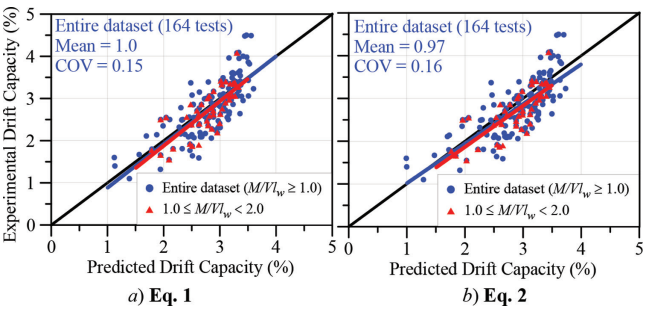

Fig. 12—Comparison of predicted drift capacity with experimental drift capacity.

SBEs do not influence (or change significantly) the lateral drift capacity. Application of linear regression analyses for the dataset of 164 tests, including the variables that significantly impact lateral drift capacity, resulted in the following predictive equation for mean drift capacity δ_c/h_w of walls with SBEs

$$\frac{\delta_c}{h_w}(\%) = 3.85 - \frac{\lambda_b}{\alpha} - \frac{v_{max}}{10\sqrt{f_c'\ \text{psi}}}$$

$$\frac{\delta_c}{h_w}(\%) = 3.85 - \frac{\lambda_b}{\alpha} - \frac{v_{max}}{0.83\sqrt{f_c'\ \text{MPa}}} \quad (1)$$

where λ_b is $l_w c/b^2$; α is 60 where overlapping hoops are used; and 45 where a combination of a single perimeter hoop with supplemental crossties is used. The first term in Eq. (1) represents the maximum mean drift capacity, whereas the second term represents the impact of c/b and l_w/b, which incorporate the influence of material properties (for example, f_y and f_c'), axial load, geometry, and quantities and distribution of longitudinal reinforcement at the boundaries and within the web, on lateral drift capacity, whereas the third term incorporates the reduction in wall drift capacity due to the level of wall shear stress normalized by the maximum shear stress allowed by ACI 318-14, Section 18.10.4.4, for an isolated wall. The drift capacities predicted with Eq. (1) are compared with experimental drift capacities in Fig. 12(a) for the entire dataset of 164 walls and for the 44 walls with $1.0 \le M/Vl_w < 2.0$. The mean and coefficient of variation (COV) are 1.0 and 0.15, respectively, over the entire range

of drift values, from roughly 1.25 to 3.5% drift. In addition, Eq. (1) was applied to the subset of 78 fully ACI 318-14 code-complaint walls identified previously, and the mean and COV of 1.03 and 0.137 are obtained, indicating that the result is not sensitive to the dataset used to derive Eq. (1). For the majority of the test specimens in the dataset, b did not vary over c (in a few cases for walls with boundary columns and thinner webs, c did extend modestly into the thinner web); however, for more complex cases, for example, biaxial loading on a flanged wall, an average or representative value of b would need to be defined to compute drift capacity. In such cases, the drift capacity is likely to be relatively large, such that this case is not critical, whereas cases with flanges in tension producing large compression on a narrow compression zone are likely to be critical.

To facilitate the implementation of Eq. (1) into design recommendations or ACI 318, Eq. (1) was simplified modestly as Eq. (2)

$$\frac{\delta_c}{h_w}(\%) = 4.0 - \frac{\lambda_b}{\alpha} - \frac{v_{max}}{10\sqrt{f_c'\,\text{psi}}} \quad (2)$$

$$\frac{\delta_c}{h_w}(\%) = 4.0 - \frac{\lambda_b}{\alpha} - \frac{v_{max}}{0.83\sqrt{f_c'\,\text{MPa}}}$$

where α is 50 where overlapping hoops are used, and 40 where a combination of a single perimeter hoop with supplemental crossties are used. The drift capacities predicted with the simplified equation (Eq. (2)) are compared with experimental drift capacities observed in Fig. 12(b) for the entire dataset of 164 walls and for the 44 walls with $1.0 \le M/Vl_w < 2.0$. The drift capacities predicted with Eq. (2) are slightly conservative, with mean and COV of 0.97 and 0.16, respectively.

CONCLUSIONS AND RECOMMENDATIONS

Based on the findings of this study, the following conclusions with regards to behavior of structural walls with SBEs can be drawn:

1. Displacement capacity of special structural walls that satisfy the detailing requirements of ACI 318-14, Section 18.10.6.4, is primarily a function of c/b, l_w/b, $v_{max}/\sqrt{f_c'}$, and use of overlapping hoops versus a single perimeter hoop with supplemental crossties. Depending on these variables, the lateral drift capacity can be as low as 1.25% and as high as 3.5%. In general, lower drift capacities result for walls with $l_w/b \ge 15$, $c/b \ge 3.0$, and wall shear stress levels approaching the ACI 318-14 limit of $10\sqrt{f_c'}$ psi ($0.83\sqrt{f_c'}$ MPa) for an individual wall.

2. ACI 318-14 Section 18.10 provisions for special structural walls do not ensure that the walls have roof drift capacity at 20% strength loss greater than the maximum roof drift demand allowed by ASCE 7-10, which is approximated as three-quarters of the allowable story drift of $0.02 \times 1.5 = 0.03$ for MCE level demands, or 0.0225. Drift capacities for a significant number of walls in the dataset are less than 0.0225.

3. A slenderness parameter, $\lambda_b = l_w c/b^2$, was defined that provides an efficient means to account for the impact of slenderness of the cross section l_w/b and the slenderness of the compression zone on the cross section c/b on wall lateral drift capacity. The slenderness parameter λ_b considers the impact of concrete and reinforcement material properties, axial load, wall geometry, and quantities and distributions of longitudinal reinforcement at the boundary and within the web.

4. The drift capacity of walls with higher shear stress ratio (that is, $v_{max}/\sqrt{f_c'}$ psi > 5 [$v_{max}/\sqrt{f_c'}$ MPa > 0.42]) is approximately 0.5% drift less than walls with low-to-moderate shear stress ratios (that is, $v_{max}/\sqrt{f_c'}$ psi ≤ 5 [$v_{max}/\sqrt{f_c'}$ MPa ≤ 0.42]). Over the full range of shear stress ratios, shear demand can reduce wall drift capacity by as much as 1.0% drift.

5. For low-to-modest shear stress ratios—that is, $v_{max}/\sqrt{f_c'}$ psi ≤ 5 ($v_{max}/\sqrt{f_c'}$ MPa ≤ 0.42), use of overlapping hoops, as opposed to use of a single perimeter hoop with supplemental crossties, provides improved drift capacity if, $c/b \ge 2.5$ or $\lambda_b \ge 40$. No clear trend of increased drift capacity is observed where overlapping hoops are used for walls with higher shear stress ratios—that is, $v_{max}/\sqrt{f_c'}$ psi > 5 ($v_{max}/\sqrt{f_c'}$ MPa > 0.42); however, given the relatively sparse data for higher shear stresses, use of overlapping hoops is recommended for all cases.

6. The drift capacity of SBEs with a single perimeter hoop and crossties with 135- to 135-degree hooks is slightly higher than for SBEs with a single perimeter hoop and crossties with alternating 90- to 135-degree hooks; however, neither is as effective as using overlapping hoops because crossties with either 90- or 135-degree hooks are prone to opening that leads to rebar buckling and crushing of the entire boundary region. Use of overlapping hoops results in an increase in drift capacity from 0.2 to 0.5% drift as λ_b increases from 40 to 100.

7. A drift capacity equation that depends on $\lambda_b = l_w c/b^2$, level of wall shear stress, and configuration of boundary transverse reinforcement was developed that accurately predicts the lateral drift capacity of walls with SBEs, with mean and coefficient of variation of approximately 1.0 and 0.15, respectively.

8. There is no real correlation between axial load ratio (ranging from 0.0 to 0.35) and wall drift capacity; therefore, limits on wall axial load (stress) alone are not recommended.

9. It is recommended that future experimental programs focus on walls with $l_w/b \ge 20$ and $c/b \ge 4$ (or walls with $\lambda \ge 80$), to address gaps in the test database given that walls with these parameters are common in practice.

AUTHOR BIOS

Saman A. Abdullah *is a PhD Candidate at the University of California, Los Angeles (UCLA), Los Angeles, CA, studying structural/earthquake engineering. He received his BS from University of Sulaimani, Kurdistan, Iraq, and his MS from California State University, Fullerton, Fullerton, CA. His research interests include seismic design of reinforced concrete structures, laboratory testing, and behavior of tall buildings.*

John W. Wallace, *FACI, is a Professor of civil engineering at UCLA. He is a member of ACI Committee 318, Structural Concrete Building Code; Seismic Provisions; 369, Seismic Repair and Rehabilitation; 374, Performance-Based Seismic Design of Reinforced Concrete Buildings; and ACI Subcommittee 318-H, Seismic Provisions. His research interests include response and design of buildings and bridges to earthquake actions, laboratory and field testing of structural components and systems, and seismic structural health monitoring.*

REFERENCES

ACI Committee 318, 1983, "Building Code Requirements for Reinforced Concrete (ACI 318-83)," American Concrete Institute, Farmington Hills, MI, 155 pp.

ACI Committee 318, 1999, "Building Code Requirements for Structural Concrete (ACI 318-99) and Commentary (ACI 318R-99), " American Concrete Institute, Farmington Hills, MI, 391 pp.

ACI Committee 318, 2014, "Building Code Requirements for Structural Concrete (ACI 318-14) and Commentary (ACI 318R-14)," American Concrete Institute, Farmington Hills, MI, 519 pp.

Architectural Institute of Japan, 2010, "AIJ Standard for Structural Calculation of Reinforced Concrete Structures," Maruzen, Tokyo, Japan. (in Japanese)

ASCE/SEI Standards, 2010, "Minimum Design Loads for Buildings and Other Structures (ASCE/SEI 7-10)," American Society for Civil Engineers, Reston, VA, 518 pp.

ASCE/SEI Standards, 2013, "Seismic Evaluation and Retrofit of Existing Buildings (ASCE/SEI 41-13)," American Society of Civil Engineers, Reston, VA, 518 pp.

Birely, A. C., 2012, "Seismic Performance of Slender Reinforced Concrete Structural Walls," PhD dissertation, University of Washington, Seattle, WA, 983 pp.

Brown, P.; Ji, J.; Sterns, A.; Lehman, D. E., Lowes; Kuchma, D.; and Zhang, J., 2006, "Investigation of the Seismic Behavior and Analysis of Reinforced Concrete Walls," *Proceedings*, 8th US National Conference on Earthquake Engineering, San Francisco, CA.

Chun, Y. S., 2015, "Seismic Performance of Special Shear Wall with the Different Hoop Reinforcement Detail and Spacing in the Boundary Element," *LHI Journal*, V. 6, No. 1, pp. 11-19. (in Korean)

Chun, Y. S.; Lee, K. H.; Lee, H. W.; Park, Y. E.; and Song, J. K., 2013, "Seismic Performance of Special Shear Wall Structural System with Effectively Reduced Reinforcement Detail," *Journal of the Korea Concrete Institute*, V. 25, No. 3, pp. 271-281. doi: 10.4334/JKCI.2013.25.3.271 (in Korean)

Chun, Y. S., and Park, J. Y., 2016, "Seismic Performance of Special Shear Wall with Modified Details in Boundary Element Depending on Axial Load Ratio," *LHI Journal*, V. 7, No. 1, pp. 31-41. (in Korean)

Eberhard, M. O., and Sozen, M. A., 1993, "Behavior-Based Method to Determine Design Shear in Earthquake-Resistant Walls," *Journal of Structural Engineering*, ASCE, V. 119, No. 2, pp. 619-640. doi: 10.1061/(ASCE)0733-9445(1993)119:2(619)

Elwood, K. J.; Maffei, J. M.; Riederer, K. A.; and Telleen, K., 2009, "Improving Column Confinement—Part 1: Assessment of Design Provisions," *Concrete International*, V. 31, No. 11, Nov., pp. 32-39.

Hines, E. M.; Seible, F.; and Priestley, M. J. N., 2002, "Seismic Performance of Hollow Rectangular Reinforced Concrete Piers with Highly Confined Corner Elements—Phase I: Flexural Tests, and Phase II: Shear Tests," *Structural Systems Research Project 99/15*, University of California, San Diego, CA, 266 pp.

Kabeyasawa, T., and Matsumoto, K., 1992, "Tests and Analyses of Ultra-High Strength Reinforced Concrete Shear Walls," *Proceedings*, 10th World Conference on Earthquake Engineering, Madrid, Spain, pp. 3291-3296.

Kabeyasawa, T.; Ohkubo, T.; and Nakamura, Y., 1996, "Tests and Analysis of Hybrid Wall Systems," *Proceedings*, 11th World Conference on Earthquake Engineering, Acapulco, Mexico.

Keintzel, E., 1990, "Seismic Design Shear Forces in RC Cantilever Shear Wall Structures," *European Earthquake Engineering*, V. 3, pp. 7-16.

Kishimoto, T.; Hosoya, H.; and Oka, Y., 2008, "Study on Structural Performance of R/C Rectangular Section Core Walls (Part 3 and 4)," *Summaries of Technical Papers of Annual Meeting*, Architectural Institute of Japan, V. C-2, pp. 355-358. (in Japanese)

Kolozvari, K.; Orakcal, K.; and Wallace, J. W., 2015, "Modeling of Cyclic Shear-Flexure Interaction in Reinforced Concrete Structural Walls. Part I: Theory," *Journal of Structural Engineering*, ASCE, V. 141, No. 5, 10 pp.

Liang, X.; Che, J.; Yang, P.; and Deng, M., 2013, "Seismic Behavior of High-Strength Concrete Structural Walls with Edge Columns," *ACI Structural Journal*, V. 110, No. 6, Nov.-Dec., pp. 953-963.

Lowes, L. N.; Lehman, D. E.; Birely, A. C.; Kuchma, D. A.; Marley, K. P.; and Hart, C. R., 2012, "Earthquake Response of Slender Concrete Planar Concrete Walls with Modern Detailing," *Engineering Structures*, V. 34, pp. 455-465.

Lu, X.; Zhou, Y.; Yang, J.; Qian, J.; Song, C.; and Wang, Y., 2010, "NEES Shear Wall Database," Network for Earthquake Engineering Simulation, Dataset, available at https://nees.org/resources/1683.

Lu, Y.; Gultom, R.; Henry, R. S.; and Ma, Q. T., 2016, "Testing of RC Walls to Investigate Proposed Minimum Vertical Reinforcement Limits in NZS 3101:2006 (A3)," *Proceedings*, 2016 NZSEE Annual Conference, Christchurch, New Zealand.

Matsubara, S.; Sanada, Y.; Tani, M.; Takahashi, S.; Ichinose, T.; and Fukuyama, H., 2013, "Structural Parameters of Confined Area Affect Flexural Deformation Capacity of Shear Walls That Fail in Bending with Concrete Crushing," *Journal of Structural and Construction Engineering*, V. 78, No. 691, pp. 1593-1602. doi: 10.3130/aijs.78.1593

Mobeen, S., 2002, "Cyclic Tests of Shear Walls Confined with Double Head Studs," MS thesis, University of Alberta, Edmoton, AB, Canada, 194 pp.

Nagae, T.; Tahara, K.; Taiso, M.; Shiohara, H.; Kabeyasawa, T.; Kono, S.; Nishiyama, M.; Wallace, J. W.; Ghannoum, W. M.; Moehle, J. P.; Sause, R.; Keller, W.; and Tuna, Z., 2011, "Design and Instrumentation of the 2010 E-Defense Four-Story Reinforced Concrete and Post-Tensioned Concrete Buildings," *PEER Report 2011/104*, Pacific Earthquake Engineering Research Center (PEER), Berkeley, CA, 234 pp.

Oesterle, R. G.; Aristizabal-Ochoa, J. D.; Fiorato, A. E.; Russell, H. G.; and Corley, W. G., 1979, "Earthquake Resistant Structural Walls–Phase II," *Report to National Science Foundation (ENV77-15333)*, Construction Technology Laboratories, Portland Cement Association, Skokie, IL, 331 pp.

Oesterle, R. G.; Fiorato, A. E.; Johal, L. S.; Carpenter, J. E.; Russell, H. G.; and Corley, W. G., 1976, "Earthquake Resistant Structural Walls—Tests of Isolated Walls," *Report to National Science Foundation (GI-43880)*, Construction Technology Laboratories, Portland Cement Association, Skokie, IL, 315 pp.

Paulay, T., and Goodsir, W. J., 1985, "The Ductility of Structural Walls," *Bulletin of the New Zealand National Society for Earthquake Engineering*, V. 18, pp. 250-269.

Segura, C. L., and Wallace, W. J., 2018a, "Seismic Performance Limitations and Detailing of Slender Reinforced Concrete Walls," *ACI Structural Journal*, V. 115, No. 3, May, pp. 849-860. doi: 10.14359/51701918

Segura, C. L., and Wallace, W. J., 2018b, "Impact of Geometry and Detailing on Drift Capacity of Slender Walls," *ACI Structural Journal*, V. 115, No. 3, May, pp. 885-896. doi: 10.14359/51702046

Seismic Engineering Research Infrastructures for European Synergies (SERIES), 2013, "SERIES RC Walls Database," available at http://www.dap.series.upatras.gr.

Seo, S.; Oh, T.; Kim, K.; and Yoon, S., 2010, "Hysteretic Behavior of RC Shear Wall with Various Lateral Reinforcements in Boundary Columns for Cyclic Lateral Load," *Journal of the Korea Concrete Institute*, V. 22, No. 3, pp. 357-366. doi: 10.4334/JKCI.2010.22.3.357

Takahashi, S.; Yoshida, K.; Ichinose, T.; Sanada, Y.; Matsumoto, K.; Fukuyama, H.; and Suwada, H., 2013, "Flexural Drift Capacity of Reinforced Concrete Wall with Limited Confinement," *ACI Structural Journal*, V. 110, No. 1, Jan.-Feb., pp. 95-104.

Thomsen, J. H. IV, and Wallace, J. W., 2004, "Displacement-Based Design of Slender Reinforced Concrete Structural Walls—Experimental Verification," *Journal of Structural Engineering*, ASCE, V. 130, No. 4, pp. 618-630. doi: 10.1061/(ASCE)0733-9445(2004)130:4(618)

Uniform Building Code, 1997, "International Council of Building Code Officials (UBC-97)," Whittier, CA.

Wallace, J. W., 1994, "A New Methodology for Seismic Design of RC Shear Walls," *Journal of Structural Engineering*, ASCE, V. 120, No. 3, pp. 863-884. doi: 10.1061/(ASCE)0733-9445(1994)120:3(863)

Wallace, J. W., 2012, "Behavior, Design, and Modeling of Structural Walls and Coupling Beams—Lessons from Recent Laboratory Tests and Earthquakes," *International Journal of Concrete Structures and Materials*, V. 6, No. 1, pp. 3-18. doi: 10.1007/s40069-012-0001-4

Wallace, J. W.; Massone, L. M.; Bonelli, P.; Dragovich, J.; Lagos, R.; Luders, C.; and Moehle, J., 2012, "Damage and Implications for Seismic Design of RC Structural Wall Buildings," *Earthquake Spectra*, V. 28, pp. 281-289. doi: 10.1193/1.4000047

Wallace, J. W., and Moehle, J. P., 1992, "Ductility and Detailing Requirements of Bearing Wall Buildings," *Journal of Structural Engineering*, ASCE, V. 118, No. 6, pp. 1625-1644. doi: 10.1061/(ASCE)0733-9445(1992)118:6(1625)

Welt, T. S., 2015, "Detailing for Compression in Reinforced Concrete Wall Boundary Elements: Experiments, Simulations, and Design Recommendations," PhD thesis, University of Illinois, Urbana-Champaign, IL, 530 pp.

Whitman, Z., 2015, "Investigation of Seismic Failure Modes in Flexural Concrete Walls Using Finite Element Analysis," MS thesis, University of Washington, Seattle, WA, 201 pp.

Xiao, Q., and Guo, Z., 2014, "Low-Cyclic Reversed Loading Test for Double-Wall Precast Concrete Shear Wall," *Journal of Southeast University*, V. 44, No. 4, pp. 826-831. (in Chinese)

Zhi, Q.; Song, J.; and Guo, Z., 2015, "Experimental Study on Behavior of Precast Shear Wall using Post-Cast at the Connection," *Proceedings*, 5th International Conference on Civil Engineering and Transportation (ICCET 2015), Guangzhou, China, pp. 1089-1092.